Performance and Greenhouse Gas Analysis of a Solar Adsorption Chiller for Canadian Residential Applications

Jordan McNally[1] and Cynthia A. Cruickshank[1]

[1] Carleton University, Ottawa (Canada)

Abstract

Space cooling makes up a significant portion of the peak electrical demand worldwide. A large electrical peak on the grid can cause fossil fuel and other non-sustainable power facilities to ramp up or turn on which produces excessive amounts of carbon dioxide. One way to reduce the cooling demand on the electrical grid is to use solar cooling technologies such as an adsorption chiller. Recent developments have allowed adsorption chillers to provide higher cooling power at lower hot water temperatures, allowing the technology to pair well with a flat plate solar collector. A performance map was generated from an experimental setup with a 16-kW silica-gel adsorption chiller and is used in a TRNSYS model to linearly determine the performance of the chiller at given inlet conditions. The adsorption chiller model was implemented into a full system model and the performance was compared among various cities in Canada. It was found that in Toronto, an adsorption system with a flat plate collector can reduce electrical consumption, annual cost of electricity, and greenhouse gas emissions from space conditioning by 40%, 49%, and 46% respectively, when compared to a system using a water to water heat pump. The adsorption system was found to be plausible in residential applications in Canada. Some future work is planned for optimizing the heat transfer to the hot water tanks from the solar collectors and chilled water storage.

Keywords: Solar cooling, adsorption chiller, modelling, residential cooling, simulation, TRNSYS.

1. Introduction

Residential space cooling demand has increased by about 170% over the past 25 years in Canada and similar trends are true around the world (Natural Resources Canada, 2017). As the demand for cooling increases so does the amount of electricity consumed, which in turn increases the peak electrical load on the grid (Proctor, 2005). Many countries, including Canada, use non-sustainable power production facilities to meet the peak electrical demand, resulting in the release of large amounts of carbon dioxide into the atmosphere. This effect is prominent in Canadian provinces during the summer months when space cooling is required. A typical breakdown of the hourly supply distribution to the Ontario grid for a weekday is shown in Figure 1.

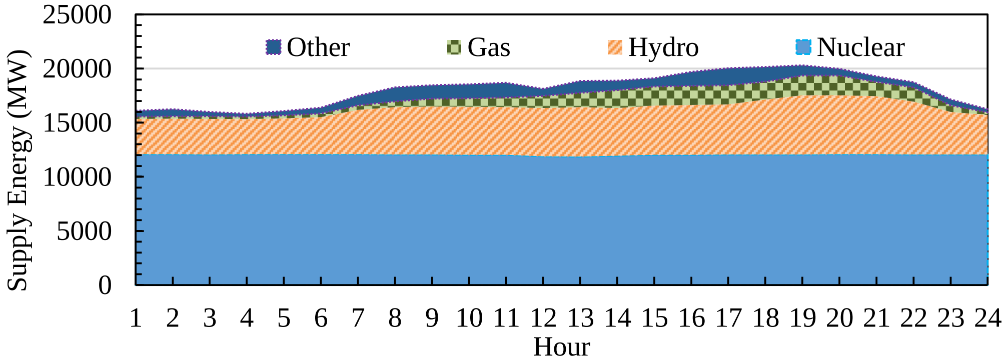

Fig. 1: Hourly electrical supply by fuel type for the Ontario grid on June 26th, 2019 (Independent Electricity System Operator, 2019)

This figure shows that during the peak and mid-peak hours (7-18) gas burning power facilities are ramped up in order to meet the increased consumption, which the nuclear and hydro facilities cannot match themselves. This electrical peak occurs during the hottest part of the day and when people are awake, meaning air conditioning is turned on and appliances are used. Solar radiance can be captured to provide the heat input to a solar cooling system, such as an adsorption chiller, which can be used to reduce this electrical peak. An adsorption chiller uses little electricity and instead uses hot water as its driving force. The hot water supply can come from district heating/waste heat or an array of solar collectors. More recently, adsorption chillers have been designed to allow them to be used with low

doi:10.18086/swc.2019.55.08 Available at http://proceedings.ises.org

temperature heat sources such as a flat plate solar collector which can supply water around 50-70°C; this is an improvement from requiring supply temperatures higher than 70°C (Bataineh and Alrifai, 2015). Additionally, in the winter months the solar collector could also be used to provide hot water to a water-source heat pump. Another benefit to reducing the peak electrical load and greenhouse gas emissions is to reduce the cost of electricity. Electrical prices are increasing at a rate where some substantial savings can be had by reducing total consumption and specifically peak consumption. The majority of Ontario, among some other provinces in Canada, use a time-of-use (TOU) billing period where the billing rate varies between on-peak, mid-peak, and off-peak depending on the period of day and when the demand is higher. Figure 2 displays the times when the peak, mid-peak, and off-peak electrical rates occur for Ontario (Ontario Hydro).

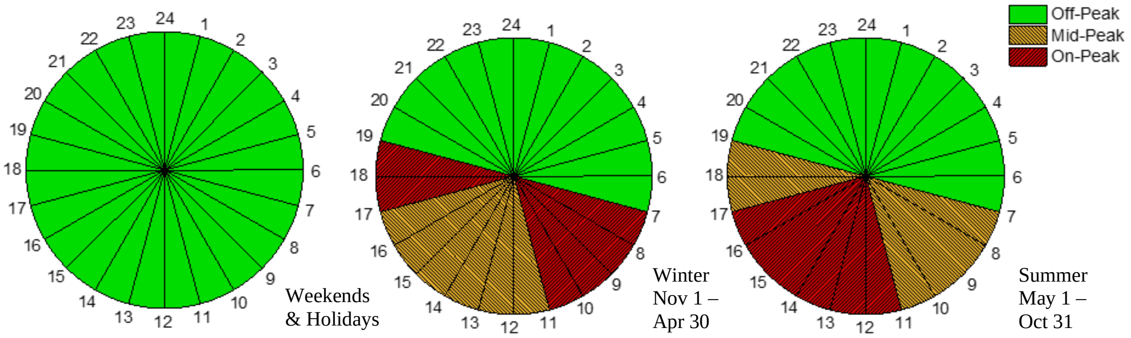

Fig. 2: Time-of-use periods for Ontario (24 Hour)

The above figure shows the winter and summer times where the electrical peak rates are billed, in red. The green represents the off-peak rates periods while yellow signifies mid-peak rates. Figure 3 shows the historical electricity rates for Ontario's TOU billing rates.

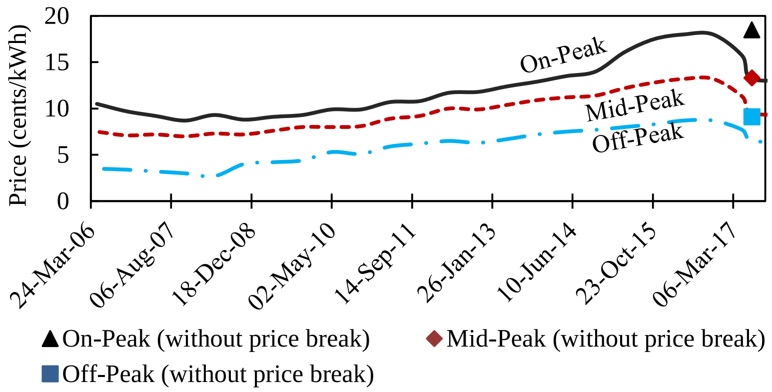

Fig. 3: Ontario electricity TOU rates from 2006-2019 (Ontario Energy Board, 2019).

The price of electricity has been increasing steadily from 2007 until a rapid increase in late 2014 where the on-demand price rapidly grew. The prices in 2016 were deemed to be too high by the provincial government so a temporary price decrease called the Fair Hydro act (Ontario Energy Board, 2017) was put into place. The reduced pricing is still in effect but changing provincial governments may remove this reduction. The points on the graph represent the projected values with no government reduction, which are expected to increase in the coming years. Any electrical savings now will only increase in the future.

Previous work has been done with silica-gel adsorption chillers where the cooling performance from constant inlet temperature tests (representative of district heating) were compared to those of dynamic inlet temperature tests (representative of solar water heating). The analysis determined that cooling power can be generated at approximately 6.5-8 kW with a COP of 0.4-0.5 for an average hot water temperature of 55-65°C (McNally et al., 2018).

This paper presents the development of a new silica-gel adsorption chiller model in TRNSYS and validation with experimental data. The model was then used to determine the cooling capabilities of an adsorption chiller with a solar water heater, cold storage tank, and hot water storage in a residential house in Toronto, Canada. Multiple configurations of the adsorption system are compared to various base cases, with and without solar collection as the main heat source. Greenhouse gas emissions and electricity costs are calculated for Toronto, and other locations have their electrical and thermal consumption compared to the Toronto model in order to illustrate the difference that weather and solar potential have on the system's performance.

2. Literature review

Solar cooling technologies have been increasing in interest in the past 15-20 years (Farenheit, 2017). The performance of this technology has also been improving in terms of efficiency, size, effectiveness of the adsorbent, and the temperature range it can operate within. The residential applications of adsorption chillers are still not fully proven in terms of reliability, performance, and cost savings. However, new models of adsorption chillers require less floor space and have greater power density. Some units can produce cooling with driving heat temperatures as low as 50°C, which is much lower when compared to the hot water temperatures required 10 years ago (65-75°C) (Bataineh and Alrifai, 2015). These improvements in adsorption cooling increase the feasibility of the technology for use in residential applications with solar water heating, and not just for industrial waste heat or district cooling applications (Bataineh and Alrifai, 2015).

Most of the solar cooling research and experimental testing has been completed within Europe as there are many government incentives for solar companies in the form of tax breaks and supplementary funding. Germany specifically, has a significant amount of companies and researchers in this field. Asia has also provided a substantial amount of research and testing of solar cooling technologies. North America, however, is a region where the research, experimental testing, and applications of adsorption cooling is lower. This could be attributed to the lack of large district heating systems and absence of strong solar cooling incentives in North America. The main differences caused by the location of testing are factors due to climate and solar irradiance. The climate and feasibility of maintaining specific inlet temperatures depend on the outdoor air in cases of heat rejection and cooling temperatures requirements. In Canada the chilled water outlet temperature does not need to be as low as a warmer region such as the middle east. The amount of heat rejection required would be lower in Canada so a cooling tower would not be needed, and a dry cooler can be used. Experimental and modelling results for solar adsorption cooling systems vary greatly depending on weather (outdoor/indoor temperature and solar irradiance) which are determined by the location.

There are studies of adsorption chillers for residential applications that have been able to quantify energy savings compared to a standard air conditioning unit; such as the study by Thomas et al. (2012) which claims a total energy savings of 40%. The chiller tested was a zeolite-water unit that has a smaller effective temperature range (55-75°C) compared to silica-gel unit at (55-95°C). This study provided a residential experimental application where an adsorption chiller system was shown to provide significant cooling with a 28 m^2 solar thermal collector array. However, like many publications this study did not have an economic analysis of the two systems, which is one area that is lacking in the literature. A model is typically needed in order to determine a comparative economic analysis between adsorption cooling systems and typical air conditioning systems.

There are various methods of modelling adsorption chillers such as a thermodynamic model, lumped parameter model, and heat and mass transfer model. The thermodynamic model is a relatively simple approach based on the steady state of the system and is useful for qualitative and semi-quantitative analysis of performance. This is the preferred method for studying the influence of temperature/heat transfer on the systems COP and cooling power. Lumped parameter models can be used to assess the transient nature of the model in more detail shown by Sah et al. (2018), and can be combined with a dynamic modelling approach to combine their strengths (Thielen et al., 2014). The heat and mass transfer approach is the most detailed modelling method and the least used due to the complex nature of the adsorption process used in Reda et al. & Schicktanz and Núñez (2016; 2009). This method uses differential equations to model the system and is the most useful approach when determining optimization design of the system (Pandit et al., 2016). Each of these approaches produce models that cannot be widely applicable to every model of adsorption chiller as the models are specific to the physical properties of each type of adsorption chiller (silica-water, silica-ammonia, zeolite-water, etc.), the internal hydraulic design, control strategy, and heat exchanger properties.

Many adsorption chiller models have been created and their results validated with an experimental setup where the goal is to optimize the adsorption chiller itself or the whole solar cooling system (sizing of thermal storage and collection) (Schicktanz and Núñez, 2009; Thielen et al., 2014). However, few models have been used for a detailed energy and economic analysis of the solar adsorption cooling system. Additionally, most models need complex inputs that are not readily available to researchers as they are manufacturer specific, such as the type and mass of the adsorbent. In this case, a model that uses experimentally determined performance maps, cycle and chiller parameters such as flow rates, max COP and cooling capacity could be useful in providing a simpler and accurate approach for producing results representative of the experimental results of a given unit.

Previous work done at Carleton University by Bowie and Cruickshank (2017) include the empirical modelling and experimental testing of a lithium-bromide absorption chiller. The experimental set up used a 5th generation absorption chiller from Climatewell rated at a cooling capacity of $10kW_{th}$. The hot water inlet range for this unit is 65-95°C. It was found this unit could only provide significant cooling with hot water inlet temperatures greater than 80°C. However, the results from this experiment should be questioned as there were issues holding a vacuum in the absorption chamber, and later the unit failed entirely. Other work at Carleton University from McNally et al. (2018) includes a study of performance of a SorTech silica-gel adsorption chiller with a rated capacity of 16 kW_{th} and a hot water inlet temperature of 55-95°C. The unit was tested using constant inlet temperatures and simulating heat input to the chiller's hot water inlet from a flat plate solar collector with an area of 24 m^2. Key results from this study will be briefly mentioned as required in this paper.

The gap in the literature for solar cooling technologies, especially for adsorption chillers is the experimental, simulation, and economical analysis of an adsorption cooling system in a Canadian climate for residential use with a flat plate solar water collector. Often models are created for the purpose of optimizing the design of an adsorption chiller, which requires precise and accurate calculations of the processes occurring within each component of the adsorption chiller. This study was conducted to determine the effects of various inlet temperatures on the COP and cooling power of a silica-gel unit with solar heating. First, a performance map from the experimental results was created. Using this performance map, the model can accurately determine inlet and outlet temperatures and illustrated how feasible these systems are for achieving residential building loads. This paper describes the modelling approach used to verify and apply a grey-box thermodynamic model of a silica-gel adsorption chiller with a solar water heater for performance analysis of residential buildings in Ontario.

3. Experimental Set-up

An experimental testing setup was created in a laboratory environment to provide a range of temperatures and flow rates (FR) to the adsorption chiller. There are three hydraulic lines connected to the adsorption chiller; a hot water line (HW), a heat rejection line (HR), and a cooled water line (AC). The hot water line is connected to a steam line through a heat exchanger, where the flow of steam is controlled by a control valve. A dry cooler capable of rejecting 40 kW at a temperature difference of 5°C is connected to the heat rejection line. The cooled water line is reheated to the inlet setpoint temperature by a heat exchanger connected to a branch off the hot water line which is also modulated by a control valve. The temperature ranges and flow rates required for the chiller are shown in Table 1. An experimental Schematic can be seen in Appendix I.

Tab. 1: Adsorption chiller specifications

Cooling Capacity (kW)	COP	HW inlet (°C)	HW FR (L/min)	HR inlet (°C)	HR FR (L/min)	AC inlet (°C)	AC FR (L/min)
16	0.65	50-95	42	22-40	80	8-22	48

The inlet and outlet temperatures for each hydraulic line are measured by T-type thermocouples. The thermocouples were all calibrated using a constant temperature bath, more details can be found in Baldwin (2013). The flow rate for each hydraulic line is measured after exiting the chiller and is assumed to be constant throughout the unit due to the integrated pumps within the chiller that make up for the pressure drop.

The experimental setup was later modified to modulate the heat input to the hot water line in order to simulate the heat input from a flat plate solar collector to test the performance of the chiller over a day using solar driven heat. A program was created that used a Canadian Weather Year for Energy Calculation dataset 2016 (CWEC) file for the Ottawa International Airport (45°19'12.0"N 75°40'12.0"W) to calculate the solar heat input that could be produced by a flat plate solar collector. The calculated solar heat input was then converted into a voltage value and sent to a proportional-integral controller that actuates the control valve and varies the heat transfer from the steam line into the hot water line.

Further details on this setup and the method for calculating the solar heat input can be found in (McNally et al., 2018). The summary of the performance of the adsorption chiller using dynamic inlet temperatures (DIT) from the above method and continuous inlet temperatures (CIT) by using a constant setpoint can be found in Figure 4. The system's setpoints are shown in Table 2.

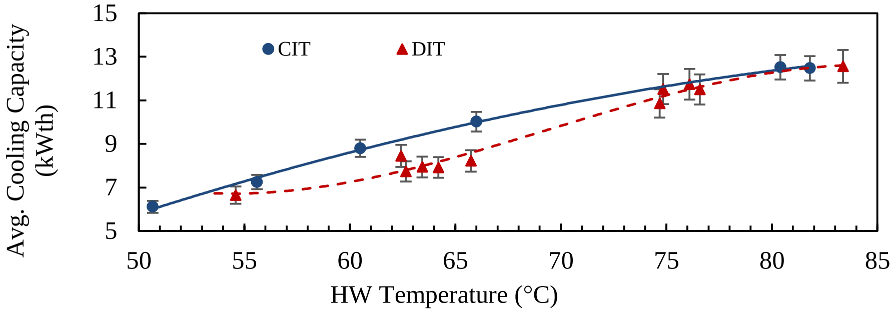

Fig. 4: CIT and DIT test results for adsorption chiller setup

Tab. 2: Testing Setpoints

HW inlet (°C)	HW FR (L/min)	HR inlet (°C)	HR FR (L/min)	AC inlet (°C)	AC FR (L/min)
81	42	27	66	24	48

Figure 4 uses two polynomial trend lines to represent the data where the CIT trendline is a second order polynomial and the DIT trendline is a cubic polynomial. The trendlines were selected based off the expected shape of the data, where the performance across the entire testing range is not linear and the increase in cooling capacity per unit of temperature increases/decreases on the low/high ranges of the HW temperature respectively. The DIT trendline uses a different polynomial because the test is averaged over a larger range of temperatures so the performance degradation on lower and higher HW temperatures are not as severe and was expected to provide lower cooling capacity in the middle, as the results showed. The SorTech adsorption chiller was tested with CIT and DIT tests with an average hot water temperature from 50-90°C. The tests show that between ~58-70°C the cooling capacity of the chiller varies from the CIT tests but with significant cooling produced. The chiller also provided significant cooling with low hot water inlet temperatures of 6-7 kW_{th} between 50-55°C. These results are promising for adsorption cooling for residential applications, especially with a flat plate solar water heater. The next step in the research was to develop a model of the adsorption chiller in order to develop a simulation system to analyze cooling and economic performance with various system setups. The following sections discusses the methodology behind the grey-box thermodynamic model of an adsorption chiller.

4. Modelling Methodology

In order to model a complex system with the very cyclic transient nature seen in adsorption chillers, a powerful simulation tool must be used. Software such as Modelica and Simulink were considered for their advanced heat and mass transfer capabilities but the Transient System Simulation Tool (TRNSYS) software was chosen due to its capabilities to add prebuilt components into the modelling environment and building load resources previously acquired. TRNSYS has an extension library called Thermal Energy System Specialists (TESS) which already has an adsorption model (Type-909) built into it based on the SJTU SWAC-10 adsorption chiller, which is about 10 years older than the unit used in this study and has a much smaller range of hot water temperatures (75-95°C) (Jakob, 2008) compared to the unit tested (50-95°C). The Type-909 component uses a thermodynamic modelling approach which requires a normalized performance map to calculate the cooling capacity and COP of the chiller. Test files containing inlet temperatures and flow rates to the adsorption chiller are also read into TRNSYS as their respective inputs for the adsorption chiller component. The mathematical workflow in the Type-909 component is as follows.

The model first checks to determine how much cooling is possible to produce by taking the lower value between the maximum cooling capacity, found from linear interpolation of the performance map for current inlet conditions, and the calculated cooling power required to reach the temperature setpoint of the chilled water line (AC), shown in Equation 1.

$$\dot{q}_{AC} = MIN\left(\dot{q}_{Capacity}, \left(\dot{m}_{AC} Cp_{AC}\left(T_{AC,in} - T_{AC,setpoint}\right)\right)\right) \qquad \text{(eq. 1)}$$

The cooling power required to reach the setpoint temperature is found by multiplying the mass flow rate, $\dot{m}$, in kg/s by the specific heat capacity for water, Cp, and the temperature difference between the AC inlet and AC setpoint, $T_{AC,setpoint}$. The cooling power produced, $\dot{q}_{AC}$, is then used to calculate the power extracted from the hot water line

(HW), shown with Equation 2.

$$\dot{q}_{HW} = \frac{\dot{q}_{AC}}{COP} \qquad \text{(eq. 2)}$$

The coefficient of performance of the chiller is linearly interpolated from the performance map to solve for the power used from the HW line. The cooling power and the heating power is then used in an energy balance for the system, as seen in Equation 3.

$$\dot{q}_{HR} = \dot{q}_{AC} + \dot{q}_{HW} + \dot{q}_{aux} \qquad \text{(eq. 3)}$$

where the heat rejection power is solved by the summation of the cooling power, hot water power, and the auxiliary power. The auxiliary power is defined as the power required to drive the pump as this accounts for thermal losses in the system. Once all the rates of power for each line are solved, the model determines the outlet temperature for each line, using Equations 4-6.

$$T_{HR,out} = T_{HR,in} + \frac{\dot{q}_{HR}}{\dot{m}_{HR}Cp_{HR}} \qquad \text{(eq. 4)}$$

$$T_{HW,out} = T_{HW,in} - \frac{\dot{q}_{HW}}{\dot{m}_{HW}Cp_{HW}} \qquad \text{(eq. 5)}$$

$$T_{AC,out} = T_{AC,in} - \frac{\dot{q}_{AC}}{\dot{m}_{AC}Cp_{AC}} \qquad \text{(eq. 6)}$$

The COP of the adsorption chiller model is determined by solving the ratio of cooling produced to the amount of heat input into the system, Equation 7, where the heat input to the system is the sum of the heat extracted from the hot water line and the thermal losses into the system from the AC pump.

$$COP = \frac{\dot{q}_{AC}}{\dot{q}_{HW}+\dot{q}_{aux}} \qquad \text{(eq. 7)}$$

Figure 5 displays the performance of the chiller over the testing ranges used for the performance map that drives this model. The incremental increase for the hot water, heat rejection, and chilled water flows were determined due to the cooling capacity and COP having a linear relation over shorter ranges of temperatures, which was determined experimentally in a previous study. The performance map was normalized to a cooling capacity of 14 kW_{th} and COP of 0.5 and transformed into a database (.dat) file for TRNSYS to use. The performance map used in the model is shown in Figure 5, where the cooling capacity is displayed on the y-axis and the chilled water temperature inlet is on the x-axis.

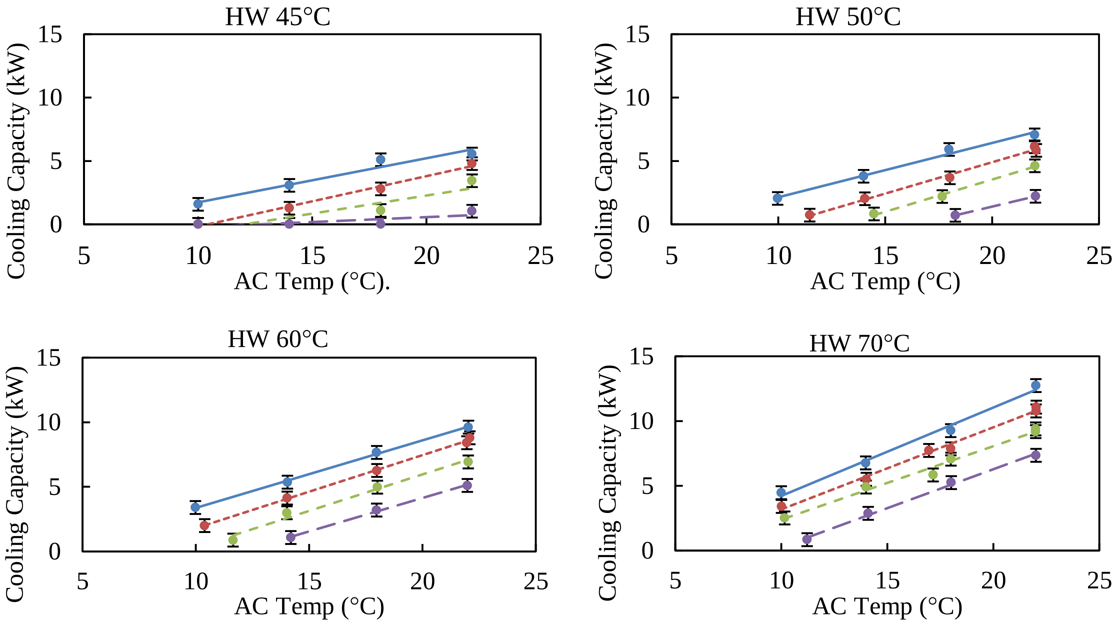

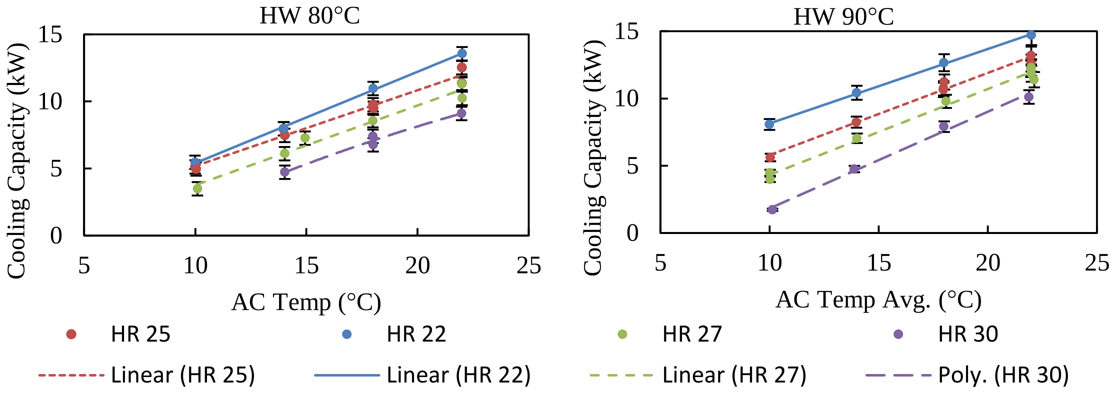

Fig. 5: Experimental adsorption chiller performance map

The data from the performance map is normalized and generated as a database file and used within TRNSYS where a TESS Type-909 is used. The Type-909 component used the performance map to linearly interpolate for the cooling performance and COP of the chiller, the COP for HW 60 is shown in Figure 6.

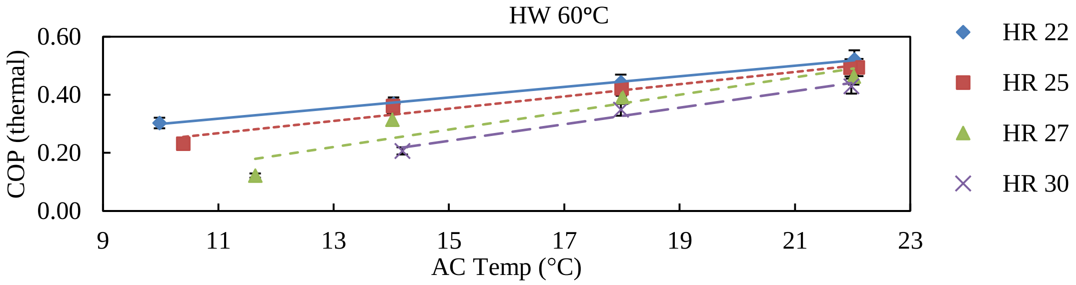

Fig 6: COP from performance map HW 60 compared to AC water temperature

The trendline for the COP data is linear as the trend for the data showed linear results, which was expected when the chiller is operated within its performance range. The linearity allowed for their values to be linearly interpolated in the TRNSYS model as previously discussed. The COP issimilar for each HR temperature when the AC temperature is higher, near 22°C, and varies at a larger range when the AC temperature is at the bottom of the range. The COP trends shown in Figure 6 remains true for the other HW temperature ranges shown by the performance maps shown in Figure 5.

5. Results

This section will provide an analysis of the adsorption model component and its comparison and validation with experimental results. Then the simulation results of the solar cooling system will be analyzed, and results from different cities and configurations will be compared.

4.1 Adsorption Model Validation

The adsorption model Type-909 in TRNSYS was used with the normalized data performance map for the adsorption chiller. When experimental input conditions were put into the model, the results matched typically within 3-12%. This is shown by integrating the total cooling, heat rejection, and heating thermal power over the test period. Numerous CIT and DIT tests were tested compared to experimentally validate the model. An example of the integrated thermal power for a CIT test can be seen in Figure 7.

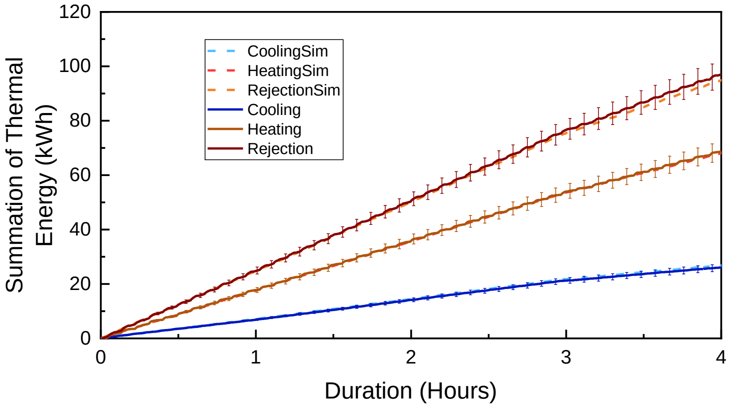

Fig. 7: Integrated simulated thermal power values for a continuous inlet temperature test (CIT)

This figure shows that each respective line falls within the error bars for the experimental data. The dotted lines are the simulation results and the solid lines are the experimental. The percent difference of the data is shown below in Table 3.

Tab. 3: Comparison of integrated thermal power between the CIT simulation and test

	Cooling (kWh$_{th}$)	Heat Rejection (kWh$_{th}$)	Heating (kWh$_{th}$)
Experimental	26.09	97.01	68.63
Simulation	26.80	94.89	68.09
Difference	0.71	2.12	0.54
%	2.71	2.18	0.79

Dynamic inlet temperature tests that simulated solar collector heat input were also conducted and the results are shown in Figure 8.

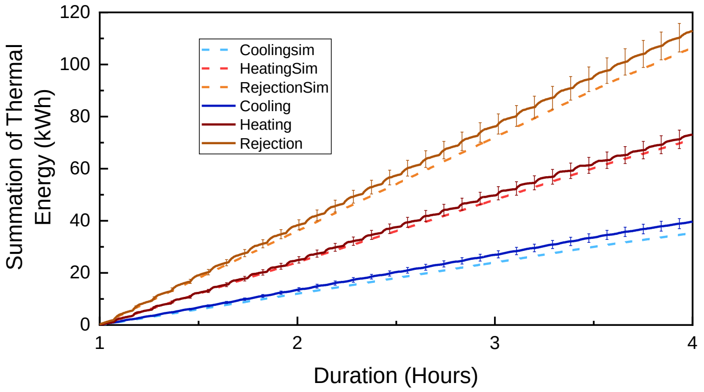

Fig. 8: Integrated thermal power for a dynamic inlet temperature test (DIT)

The integrated results for the DIT fall outside the error bars of the experimental results but are still within 12%. Table 4 shows the numerical details on the accuracy for Figure 8.

Tab. 4: Comparison of integrated thermal power between DIT simulation and test

	Cooling (kWhth)	Heat Rejection (kWhth)	Heating (kWhth)
Experimental	39.70	112.90	73.08
Simulation	35.25	106.41	71.16
Difference	4.44	6.49	1.92
Difference/Experimental	0.11	0.06	0.03
%	11.20	5.75	2.63

4.2 Adsorption System Simulation

A previously developed and validated house model for a standard newly built home in urban Ontario by Baldwin and Cruickshank (2016) was used and modified for this study. The house modelled is a two story, single detached home with a basement. The house has a total floor area of 330 m^2 divided evenly between the 3 floors. Each of the floors were divided into their own thermal zones as well as the attic. A single thermostat is located on the main floor with the heating and cooling setpoint of 20°C and 23°C respectively. Further details can be found in their publication. The model was modified to support the various methods of heating and cooling used to make up the different test cases shown in Table 5.

Tab. 5: Cases for simulation tests

Case 1	Heat pump for heating and cooling
Case 2	Electrical heater and standard AC
Case 3	Natural gas burning furnace and standard AC
Case 4	Adsorption chiller and heat pump with constant hot water supply (const. HW)
Case 5	Adsorption chiller with 39.2 m^2 solar collector, 500 L tank and heat pump with (const. HW)
Case 6	Adsorption chiller with 39.2 m^2 solar collector 500 L tank and heat pump with solar collector

The system diagram for some of these cases can be seen in Appendix II. These cases were selected based on what HVAC equipment can typically be found in homes in Canada both old and new, with the addition of the adsorption chiller cases (Cases 4-6). The electrical consumption or fuel consumption for the constant hot water supply is not considered for any of the cases. It should be noted that on a district heating system hot water supply would be readily available but if this is not the case there would be added electricity consumption and GHG emissions produced for Case 1, Case 4, and Case 5. The thermal and electrical consumption for each of these cases in Toronto are shown in Figure 9.

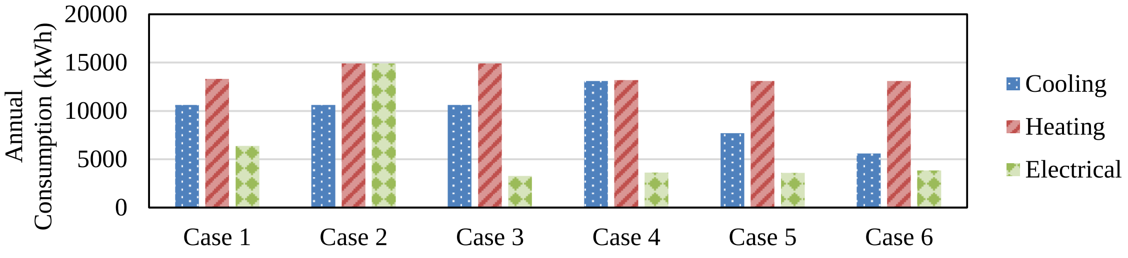

Fig. 9: Simulated annual thermal and electrical consumption for house model in Toronto

The cooling load produced from the adsorption chiller in Case 5 and Case 6 are lower and could be seen as undersized, however the temperatures in the house are still conditioned in such a manner that would be considered comfortable according to ASHRAE standards with the maximum temperature in the summer under 27°C. The average and mean main floor temperature during the cooling season is 21.81°C and 21.77°C for the Base Case and 21.43°C and 21.42°C for Case 6, respectively. Case 4 shows how the chiller would provide higher hot water temperatures and that the electrical consumption does not increase when compared to Case 6. Figure 10 shows the electrical consumption for each peak rate for the TOU billing for each case.

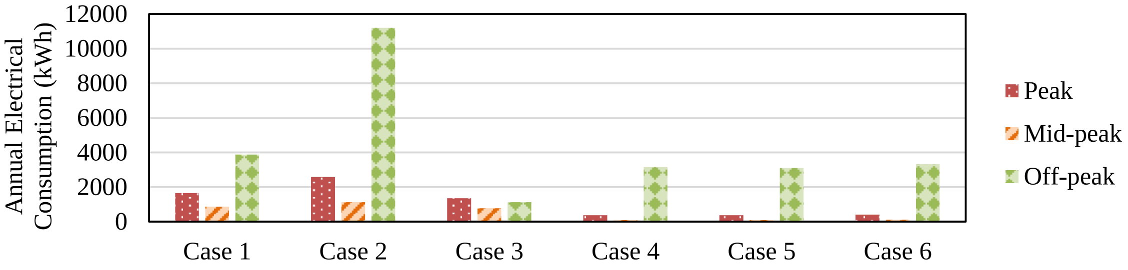

Fig. 10: Simulated annual electrical consumption breakdown by time-of-use rate

The adsorption systems significantly reduce the peak electrical consumption when most of the peak is comprised of the cooling load. Additionally, the electric heating in Case 2 affects the peak load less and affects the off-peak load more than the respective adsorption cases. The off-peak period is still similar which is due to the heating being provided by the same heat pump. In comparison to a standard AC and electric heating the adsorption and heat pump system for cooling and heating require significantly less energy. The greenhouse gas emissions in terms of equivalent

CO_2 and cost of each case is shown in Figure 11.

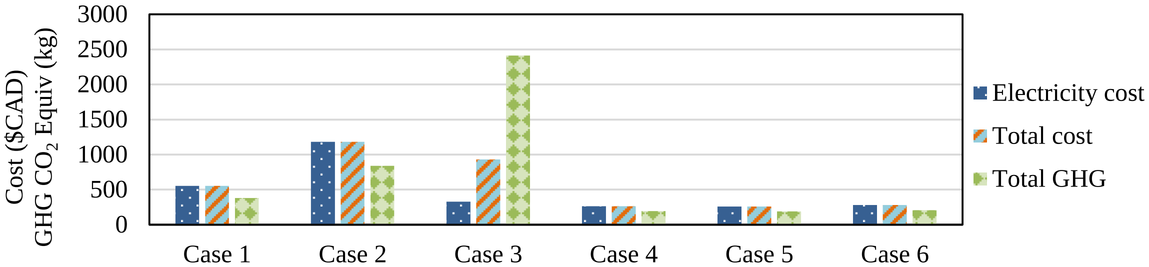

Fig. 11: Economic and environmental costs/impacts for each experimental case in Toronto

Natural gas heating is cheaper than that of an electric heater but produces significantly more greenhouse gases in Ontario; as is illustrated in Figure 11. The cost of electricity between adsorption cases and the first three cases is significantly reduced. This is mostly due to the reduction in the need of large amounts of power to cool the house. The electricity cost of the Cases 4-6 won't increase greatly if the cooling produced is increased but remain the same. To increase the amount of cooling produced a larger solar array or cooling storage would be required.

Other cities around Canada were tested to show the systems performance in various climates with varying average temperatures and precipitation. The cities tested were Vancouver, Saskatoon, Toronto, Ottawa, Montreal, and Halifax. These tests were only conducted for the Case 1, Case 3, and Case 6. The comparison of the cooling power, heating power, and electricity consumed for all these cities are shown in Figures 12-14.

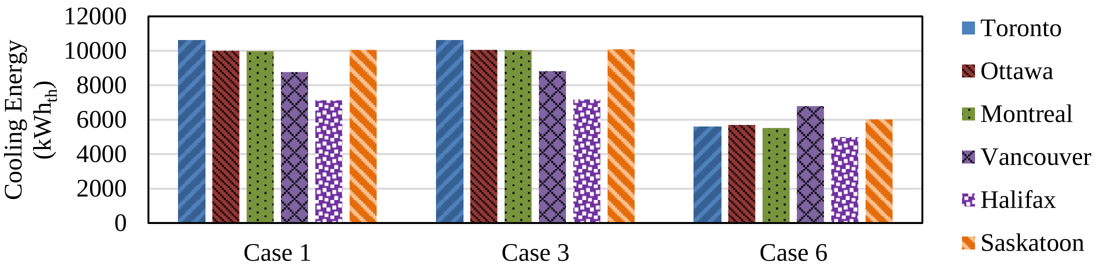

Fig. 12: Simulated annual cooling energy consumed for model in Canadian cities

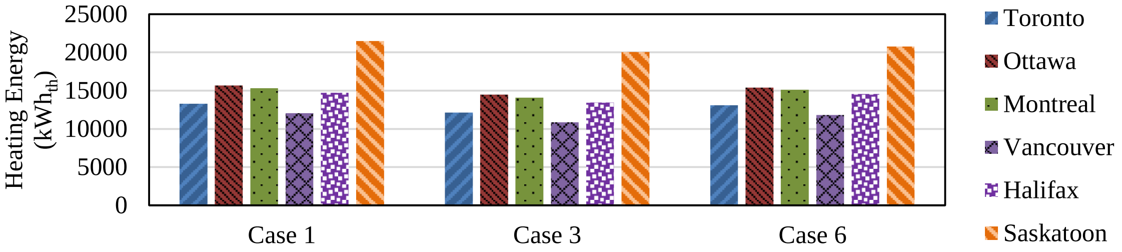

Fig. 13: Simulated annual heating energy consumed for model in Canadian cities

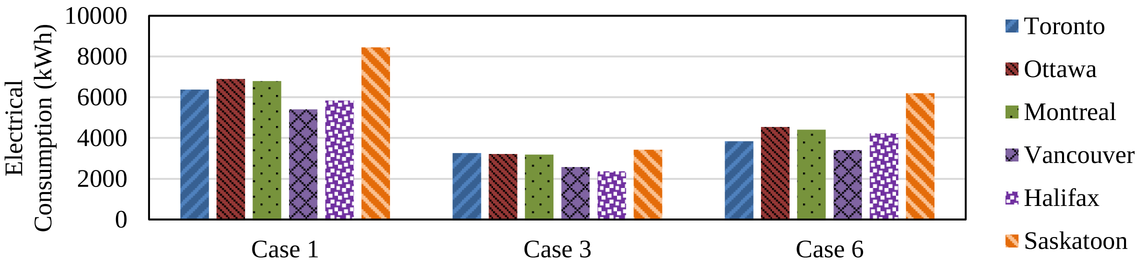

Fig. 14: Simulated annual electricity consumption for model in Canadian cities

This set of results show how various ambient temperatures, precipitation, and solar irradiance affect the solar cooling system. These results show that an adsorption chiller paired with a flat plate collector and a heat pump with the heat source connected to a flat plate collector allows the heating/cooling system to reduce the total electrical consumption in every city it was applied in. The heating provided was sufficient when the heat source for the heat pump was the flat plate collector. Although the cooling provided in Case 3 was lesser than the base case, it was still significant and enough to provide a comfortable living environment, showing the capability of adsorption cooling in Canada.

6. Conclusion

An experimental setup with a 16-kW adsorption chiller was tested, and the cooling capacity and temperature relationship was proven to be linear across the operational range. This allowed for a performance map to be generated and linear interpolation to be used between the tested points. TRNSYS was used to develop a model for the purpose of determining the performance of an adsorption chiller in various residential applications in Ottawa, Canada. The TRNSYS TESS component Type-909 for adsorption chillers was found to be representative of the tested adsorption chiller's integrated heat transfer over test periods. This allowed the adsorption chiller model of the experimental unit to be used with a validated house model. The house model was then modified for different cases of heating and cooling configurations with heat pumps, standard air conditioners, flat plate collectors, and adsorption chillers. It was found that adsorption cooling driven by a flat plate collector which was also hooked up to the heat pump reduced electrical consumption while providing significant cooling. The limiting factor in the system is the temperature of the hot water tank, where a constant temperature of 75°C would have provided cooling potential equivalent to that of the Base Case.

Future work is needed to optimize the system in order to maximize the temperature of the hot water tank and size a cold-water tank with a control strategy. A full system optimization will be completed, and the economic and environmental analysis will be expanded to include other provinces and the cost of system components. This study was preliminary work to show the potential GHG reductions and reduction in energy demand. Some future work will be to determine full system costs, payback period, and other economic feasibility metrics.

7. References

Baldwin, C., 2013. Design and Construction of an Experimental Apparatus to Assess the Performance of a Solar Absorption Chiller with Integrated Thermal Storage. Carleton University. https://doi.org/https://doi.org/10.22215/etd/2014-10066

Baldwin, C., Cruickshank, C.A., 2016. Assessing the Potential for Reduction in Peak Residential Electrical Loads Using a Heat Pump and Thermal Storage. Int. Compress. Eng. Refrig. Air Cond. High Perform. Build. Conf. 1–10.

Bataineh, K.M., Alrifai, S., 2015. Recent trends in solar thermal sorption cooling system technology. Adv. Mech. Eng. 7, 1–20. https://doi.org/10.1177/1687814015586120

Bowie, D., Cruickshank, C.A., 2017. Experimental evaluation of a triple-state sorption chiller. Int. J. Refrig. 81, 12–25. https://doi.org/10.1016/j.ijrefrig.2017.05.009

Farenheit, 2017. Cooling Innovation. Tech. Inf. Sheet.

Independent Electricity System Operator, 2019. Power Data [WWW Document]. URL http://www.ieso.ca/power-data

Jakob, U., 2008. Overview on Small Capacity Systems, in: OTTI International Solar Air-Conditioning Seminar. SolarNext AG, Rimsting, Germany.

McNally, J., Baldwin, C., Cruickshank, C.A., 2018. Using Adsorption Cooling and Thermal Solar Collection for Residential Cooling Applications in Canada, in: Volume 6A: Energy. ASME, p. V06AT08A045. https://doi.org/10.1115/IMECE2018-87246

Natural Resources Canada, 2017. Energy Use Data Handbook: 1990 - 2014.

Ontario Energy Board, 2019. Historical electricity rates [WWW Document]. URL https://www.oeb.ca/rates-and-your-bill/electricity-rates/historical-electricity-rates (accessed 3.17.19).

Ontario Energy Board, 2017. Electricity prices are dropping again on July 1 [WWW Document]. URL https://www.oeb.ca/newsroom/2017/electricity-prices-are-dropping-again-july-1 (accessed 3.17.19).

Ontario Hydro, n.d. Ontario Hydro Rates [WWW Document]. URL http://www.ontario-hydro.com/current-rates

Pandit, D., Choudhury, B., Sarkar, J.P., 2016. Modelling Analysis of Silica Gel / Water Adsorption Chiller Systems : A Review. Int. J. Res. Sci. Innov. III, 18–26.

Proctor, J., 2005. Air Conditioning , Peak Demand , And Public Goods Funds 94901.

Reda, A.M., Ali, A.H.H., Morsy, M.G., Taha, I.S., 2016. Design optimization of a residential scale solar driven adsorption cooling system in upper Egypt based. Energy Build. 130, 843–856. https://doi.org/10.1016/j.enbuild.2016.09.011

Sah, R.P., Choudhury, B., Das, R.K., 2018. Study of a two-bed silica gel–water adsorption chiller: performance analysis. Int. J. Sustain. Energy 37, 30–46. https://doi.org/10.1080/14786451.2016.1173696

Schicktanz, M., Núñez, T., 2009. Modelling of an adsorption chiller for dynamic system simulation. Int. J. Refrig. 32, 588–595. https://doi.org/10.1016/j.ijrefrig.2009.02.011

Thielen, N., Bardow, A., Bau, U., Graf, S., Schreiber, H., Lanzerath, F., Gräber, M., 2014. Adsorption energy systems library - Modeling adsorption based chillers, heat pumps, thermal storages and desiccant systems. Proc. 10th Int. Model. Conf. March 10-12, 2014, Lund, Sweden 96, 875–883. https://doi.org/10.3384/ecp14096875

Thomas, S., Hennaut, S., Maas, S., Andre, P., 2012. Experimentation and simulation of a small-scale adsorption cooling system in temperate climate. Energy Procedia 30, 704–714. https://doi.org/10.1016/j.egypro.2012.11.080

8. Appendix

Appendix I

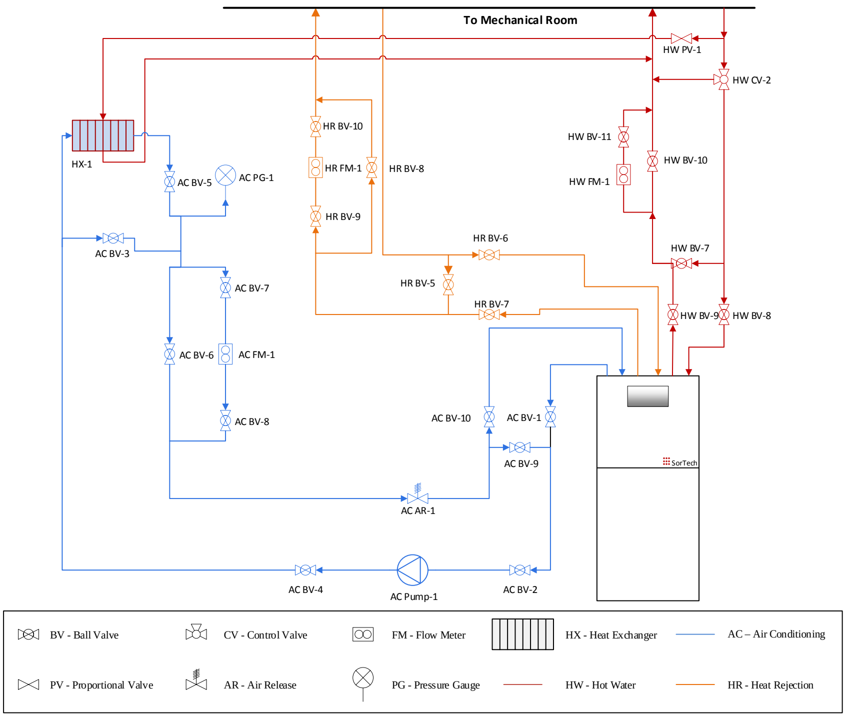

Appendix II

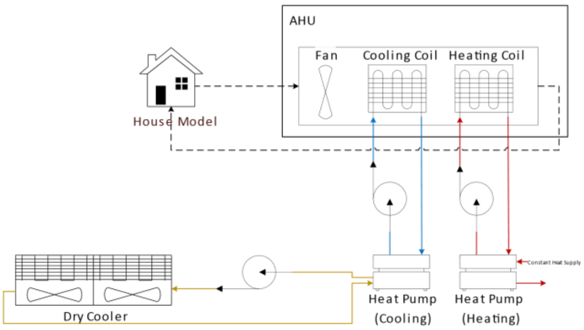

Figure 15: Base case schematic

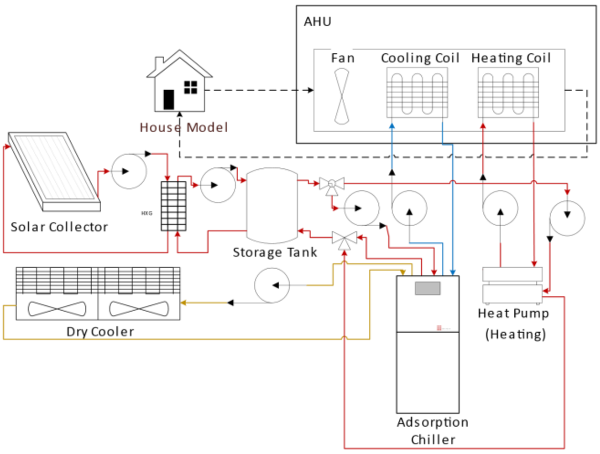

Figure 16: Case 3 system schematic